A Precise Measurement of the Muon Neutrino-Nucleon Inclusive Charged Current Cross-Section off an Isoscalar Target in the Energy Range $2.5 < E_\nu < 40$ GeV by NOMAD

Q. Wu [s] S.R. Mishra [s] A. Godley [s] R. Petti [s] S. Alekhin [y]
P. Astier [n] D. Autiero [h] A. Baldisseri [r] M. Baldo-Ceolin [m]
M. Banner [n] G. Bassompierre [a] K. Benslama [i] N. Besson [r]
I. Bird [h,i] B. Blumenfeld [b] F. Bobisut [m] J. Bouchez [r] S. Boyd [t]
A. Bueno [c,x] S. Bunyatov [f] L. Camilleri [h] A. Cardini [j]
P.W. Cattaneo [o] V. Cavasinni [p] A. Cervera-Villanueva [h,v]
R. Challis [k] A. Chukanov [f] G. Collazuol [m] G. Conforto [h,u,1]
C. Conta [o] M. Contalbrigo [m] R. Cousins [j] H. Degaudenzi [i]
T. Del Prete [p] A. De Santo [h,p] L. Di Lella [h,2]
E. do Couto e Silva [h] J. Dumarchez [n] M. Ellis [t] G.J. Feldman [c]
R. Ferrari [o] D. Ferrère [h] V. Flaminio [p] M. Fraternali [o]
J.-M. Gaillard [a] E. Gangler [h,n] A. Geiser [e,h] D. Geppert [e]
D. Gibin [m] S. Gninenko [h,ℓ] J.-J. Gomez-Cadenas [h,v] J. Gosset [r]
C. Gößling [e] M. Gouanère [a] A. Grant [h] G. Graziani [g]
A. Guglielmi [m] C. Hagner [r] J. Hernando [v] P. Hurst [c] N. Hyett [k]
E. Iacopini [g] C. Joseph [i] F. Juget [i] N. Kent [k] J.J. Kim [s]
M. Kirsanov [ℓ] O. Klimov [f] J. Kokkonen [h] A. Kovzelev [ℓ,o]
A. Krasnoperov [a,f] S. Kulagin [ℓ] S. Lacaprara [m] C. Lachaud [n]
B. Lakić [w] A. Lanza [o] L. La Rotonda [d] M. Laveder [m]
A. Letessier-Selvon [n] J.-M. Levy [n] J. Ling [s] L. Linssen [h]
A. Ljubičić [w] J. Long [b] A. Lupi [g] V. Lyubushkin [f]
A. Marchionni [g] F. Martelli [u] X. Méchain [r] J.-P. Mendiburu [a]
J.-P. Meyer [r] M. Mezzetto [m] G.F. Moorhead [k] D. Naumov [f,g]
P. Nédélec [a] Yu. Nefedov [f] C. Nguyen-Mau [i] D. Orestano [q]
F. Pastore [q] L.S. Peak [t] E. Pennacchio [u] H. Pessard [a] A. Placci [h]
G. Polesello [o] D. Pollmann [e] A. Polyarush [ℓ] C. Poulsen [k]
B. Popov [f,n] L. Rebuffi [m] J. Rico [x] P. Riemann [e] C. Roda [h,p]

A. Rubbia [h,x] F. Salvatore [o] O. Samoylov [f] K. Schahmaneche [n]
B. Schmidt [e,h] T. Schmidt [e] A. Sconza [m] M. Seaton [s] M. Sevior [k]
D. Sillou [a] F.J.P. Soler [h,t] G. Sozzi [i] D. Steele [b,i] U. Stiegler [h]
M. Stipčević [w] Th. Stolarczyk [r] M. Tareb-Reyes [i] G.N. Taylor [k]
V. Tereshchenko [f] A. Toropin [ℓ] A.-M. Touchard [n] S.N. Tovey [h,k]
M.-T. Tran [i] E. Tsesmelis [h] J. Ulrichs [t] L. Vacavant [i]
M. Valdata-Nappi [d,3] V. Valuev [f,j] F. Vannucci [n] K.E. Varvell [t]
M. Veltri [u] V. Vercesi [o] G. Vidal-Sitjes [h] J.-M. Vieira [i]
T. Vinogradova [j] F.V. Weber [c,h] T. Weisse [e] F.F. Wilson [h]
L.J. Winton [k] B.D. Yabsley [t] H. Zaccone [r] K. Zuber [e]
P. Zuccon [m]

[a] LAPP, Annecy, France
[b] Johns Hopkins Univ., Baltimore, MD, USA
[c] Harvard Univ., Cambridge, MA, USA
[d] Univ. of Calabria and INFN, Cosenza, Italy
[e] Dortmund Univ., Dortmund, Germany
[f] JINR, Dubna, Russia
[g] Univ. of Florence and INFN, Florence, Italy
[h] CERN, Geneva, Switzerland
[i] University of Lausanne, Lausanne, Switzerland
[j] UCLA, Los Angeles, CA, USA
[k] University of Melbourne, Melbourne, Australia
[ℓ] Inst. for Nuclear Research, INR Moscow, Russia
[m] Univ. of Padova and INFN, Padova, Italy
[n] LPNHE, Univ. of Paris VI and VII, Paris, France
[o] Univ. of Pavia and INFN, Pavia, Italy
[p] Univ. of Pisa and INFN, Pisa, Italy
[q] Roma Tre University and INFN, Rome, Italy
[r] DAPNIA, CEA Saclay, France
[s] Univ. of South Carolina, Columbia, SC, USA
[t] Univ. of Sydney, Sydney, Australia
[u] Univ. of Urbino, Urbino, and INFN Florence, Italy
[v] IFIC, Valencia, Spain
[w] Rudjer Bošković Institute, Zagreb, Croatia
[x] ETH Zürich, Zürich, Switzerland
[y] Inst. for High Energy Physics, 142281, Protvino, Moscow, Russia

Abstract

We present a measurement of the muon neutrino-nucleon inclusive charged current cross-section, off an isoscalar target, in the neutrino energy range $2.5 \leq E_\nu \leq 40$ GeV. The significance of this measurement is its precision, $\pm 4\%$ in $2.5 \leq E_\nu \leq 10$ GeV, and $\pm 2.6\%$ in $10 \leq E_\nu \leq 40$ GeV regions, where significant uncertainties in previous experiments still exist, and its importance to the current and proposed long baseline neutrino oscillation experiments.

1 Motivation

The muon neutrino-nucleon inclusive charged current (ν_μ-N CC) cross-section has been well measured at high neutrino energies ($30 \leq E_\nu \leq 250$ GeV), primarily by the CCFR [1] and the CDHSW [2] experiments. The average absolute ν_μ-N CC cross-section, where 'N' is a nucleon in an isoscalar target, above E_ν of 30 GeV, $\sigma^{CC}(\nu_\mu N) = (0.677 \pm 0.014)E_\nu \ cm^2/\text{GeV}$, is measured to a 2.1% precision. In contrast the $\sigma^{CC}(\nu_\mu N)$ is imprecisely measured below 30 GeV. Previous measurements are shown in Figure 3 and summarised in [3]. Accurate determination of $\sigma^{CC}(\nu_\mu N)$ below E_ν of 30 GeV is of interest in its own right, and offers insight into CC processes such as quasi-elastic and resonance interactions, and their transition into the deep inelastic scattering region. The current and the proposed long baseline neutrino experiments, such as MINOS and NOνA at Fermilab and T2K in Japan, address the atmospheric ν oscillations at the mass-difference, $\Delta m_{23}^2 \approx 2.5 \times 10^{-3}$ eV^2. Given their typical flight path of a few hundred kilometers, they use neutrino beams with energies well below 30 GeV. Cross sections in this region should be precisely known to accurately interpret the results of these experiments. The NOMAD data are suitable for such a precision $\sigma^{CC}(\nu_\mu N)$ measurement due to the large ν-interaction sample, good low-energy resolution and a ν_μ flux which spans $\mathcal{O}(1) \leq E_\nu \leq 300$ GeV with a mean energy of 24.3 GeV.

---

[1] Deceased
[2] Now at Scuola Normale Superiore, Pisa, Italy
[3] Now at Univ. of Perugia and INFN, Perugia, Italy

2 The Beam and the Detector

The Neutrino Oscillation MAgnetic Detector (NOMAD) experiment at CERN used a neutrino beam produced by the 450 GeV SPS-protons striking a beryllium target and producing secondary $\pi^\pm$, $K^\pm$, and K_L^0 mesons. The positively charged mesons were focussed by a system of collimators, a magnetic horn and a reflector into a 290 m long evacuated decay pipe. Decays of $\pi^\pm$, $K^\pm$, and K_L^0 produced the SPS neutrino beam. The average flight path of the neutrinos to the NOMAD was 628 m; the detector being 836 m downstream of the Be-target. The SPS beamline and the neutrino flux incident at NOMAD are described in [4] and [5].

NOMAD was designed to search for $\nu_\mu \rightsquigarrow \nu_\tau$ oscillations at $\Delta m^2 \geq 5$ eV^2, and in this Δm^2 range it set the current best limit on this search [6]. The experiment recorded over 1.7 million neutrino interactions in its active drift-chamber (DC) target. These data are unique in that they constitute the largest high resolution neutrino data sample with accurate identification of ν_μ, $\overline{\nu}_\mu$, ν_e, and $\overline{\nu}_e$ in the energy range $\mathcal{O}(1) \leq E_\nu \leq 300$ GeV. In addition, upstream of the active-DC target, the experiment recorded over 2 million ν-interactions in the Al-coil, and over 20 million in the Fe-scintillator calorimeter (FCAL).

The NOMAD apparatus, described in [7], was composed of several sub-detectors. The active target comprised 132 planes of 3×3 m^2 drift chambers with an average density similar to that of liquid hydrogen (0.1 gm/cm^3) [8]. On average, the equivalent material in the DC encountered by particles produced in a ν-interaction was about 0.5 X_0 and a quarter of an interaction length (λ). The fiducial mass of the NOMAD DC-target, composed primarily of carbon (64%), oxygen (22%), nitrogen (6%), and hydrogen (5%), was 2.7 tons. The measured composition of the target was 52.43% protons and 47.57% neutrons. The correction for non-isoscalarity was about 5%. Downstream of the DC, there were nine modules of transition radiation detectors (TRD), followed by a preshower (PRS) and a lead-glass electromagnetic calorimeter (ECAL). The ensemble of DC, TRD, and PRS/ECAL was placed within a dipole magnet providing a 0.4 T magnetic field. Outside the magnet was a hadron calorimeter (HCAL), followed by two muon-stations comprising large area drift chambers separated by an iron filter. The two muon-stations, placed at 8- and 13-λ downstream of the ECAL, provided a clean identification of the muons.

The charged tracks in the DC were measured with an approximate momentum (p) resolution of $\sigma_p/p = 0.05/\sqrt{L} + 0.008p/\sqrt{L^5}$, p in GeV and L in meters, with unambiguous charge separation in the energy range of interest. The π^0 component of the ν-hadronic jet was measured by the ECAL with a resolution of $\sigma_E/E = 3.2\%/\sqrt{E} + 1\%$. The detailed individual reconstruction of each charged and neutral track and their precise momentum vector measurement

enabled a quantitative description of the event kinematics: the strength and basis of NOMAD analyses. In a ν_μ-CC interaction, in addition to the three traditional variables, energy (E_μ), angle (θ_μ) of the emergent muon, and the hadron energy (E_{HAD}), the detector uniquely offered a measurement of the missing transverse momentum $(\not{p}_T)$ vector in a plane transverse to the neutrino direction.

3 The Analysis

The $\sigma^{CC}(\nu_\mu N)$ was measured by dividing the fully corrected ν_μ-CC data by the corresponding ν_μ-flux as a function of E_ν. We first describe the measurement of the numerator. In a ν_μ-CC interaction, the neutrino energy (E_ν) was measured by adding the energies of the muon (E_μ) and particles composing the hadron-jet (E_{HAD}) yielding the total visible energy (E_{VIS}) of the interaction. The observed CC-data, binned in E_ν commensurate with resolution and statistics, were corrected for the detector acceptance, the efficiency of the cross section selection cuts, and the reconstruction smearing effects using ν_μ-CC Monte Carlo (MC) samples.

To produce a clean sample of ν_μ-CC events, the following selection criteria were imposed. Since the $\sigma^{CC}(\nu_\mu N)$ analysis was entirely dominated by systematic errors, more stringent fiducial cuts were imposed than those used in statistical-error limited analyses such as [6].

Next, a successful match between a drift chamber track to track-segments in both muon chambers yielded the muon identification (μ-ID). The polar angle of the muon with respect to the incident neutrino direction, θ_μ, was required to be less than 0.5 radians. The $P_\mu > 2.5$ GeV cut, dictated by the thickness of the HCAL preceding the first muon station, defined the low energy limit of our measurement. Finally, for the 1-track sample a cut on the transverse muon-momentum, $p_t^2 = (P_\mu \times \theta_\mu)^2 > 0.0025$ GeV^2, was used to eliminate the inverse muon decay events with minimal loss of efficiency.

The standard NOMAD ν-event generator, NEGLIB, and the detailed Monte Carlo simulation was based upon LEPTO 6.1 [9] and JETSET [10] generators for neutrino interactions and on a GEANT [11] based program for the detector response. The parton content of the nucleon were taken from Ref. [12]. The ν_μ-MC included deep-inelastic scattering (DIS), resonance (RES), and quasi-elastic (QE) processes. The relative abundance of DIS:RES:QE samples, averaged over the ν_μ-flux, was taken to be 1.0:0.031:0.024. The (QE+RES) to DIS, and QE to RES, cross sections were separately varied by $\pm15\%$ and the resulting small difference in $\sigma^{CC}(\nu_\mu N)$ was taken as a systematic error. The acceptance computed using the total number of generated MC in the standard

Cut	Data	QE	RES	DIS	ν_μ-CC	NC	ν_e	$\overline{\nu}_e$	$\overline{\nu}_\mu$
Generated in Fid		32198.8	42869.7	1364812.4	1439880.9	547103.1	21598.3	2159.9	35996.0
Reconstructed	4022549.0	27985.2	37120.5	1182505.1	1247610.9	394053.7	18905.1	1881.3	31033.7
Fiducial Volume	1815455.0	20265.1	31040.1	1122888.6	1174193.9	313487.8	18131.8	1547.6	27201.8
Negative Muon	1069609.0	20114.0	30816.5	987008.8	1037939.3	6707.8	325.5	24.1	279.4
Quality Cuts	1043691.0	19960.3	30527.3	985255.8	1035743.3	6698.7	325.5	24.1	279.3
$E_\mu > 2.5$	1038783.0	19941.9	30509.7	980265.8	1030717.4	6484.5	316.0	23.2	270.0
$\theta_\mu < 0.5\ rad$	1035260.0	19939.4	30503.0	978387.4	1028829.8	6476.8	314.8	23.1	267.9
$p_t^2 > 0.0025$	1035107.0	19906.7	30472.9	978383.2	1028762.8	6476.8	314.8	23.1	267.9

Table 1

Selection Criteria for ν_μ Charged Current Events: The numbers of Data, and normalized MC samples from ν_μ-CC, NC, and ν_e-, $\overline{\nu}_e$-, and $\overline{\nu}_\mu$-CC events passing the $\sigma^{CC}(\nu_\mu N)$ analysis cuts are shown.

NOMAD fiducial volume [6] and the corresponding number of reconstructed MC events passing event selection cuts took into account the bias in the true average energy due to the event reconstruction and selection process. It should be noted that the standard NOMAD fiducial volume used for generated MC (the denominator in acceptance calculation) was about 22% larger than that used for the reconstructed sample. A small impurity (0.7%) due to neutral-current (NC), from ν and $\overline{\nu}$ interactions, induced μ^--sample was corrected using the NC-MC estimation. The effects of the selection cuts on data and Monte Carlo are summarized in Table 1.

4 The ν_μ-Flux and the Absolute Normalization

Cross-section measurements require a knowledge of the ν-flux. Neutrinos in the SPS beam were mainly from π, K, and μ decays. The uncertainty in modeling these secondary particles, and hence the ν-flux, was — and for all the $\sigma^{CC}(\nu_\mu N)$ measurements has been — the dominant source of systematic error. Fortunately for NOMAD, a dedicated measurement of π/K yields in 450 GeV p-Be collision at various secondary energies and angles was undertaken by the SPY experiment [13]. The SPY measurement of the $\pi^\pm/K^\pm$ yields was carried out at discrete energies spanning 7 to 135 GeV, and a detailed transverse-momentum (P_T) scan at 15 and 40 GeV that were especially useful to the present measurement. A previous measurement of π/K yield in a 400 GeV p-Be collision by Atherton et al. [14] was also used in the ν-flux determination. Other systematic uncertainties in the ν_μ-flux determination arose from the variation in the position of the primary proton beam and the simulation of the propagation of secondaries through the beam line. The energy dependent relative ν_μ flux errors [5] were the largest source of systematic error in this analysis.

In this analysis only the relative ν_μ-flux, i.e. number of ν_μ in E_ν bins, obtained using the SPY/Atherton measurements, was used. The absolute normalization of the ν_μ-flux was fixed using the world average of $\frac{\sigma(\nu N)}{E}$ above 40 GeV. The absolute flux normalisation was computed in the following energy regions: 40-100 GeV, 40-150 GeV, 50-150 GeV, and 50-200 GeV. Variations in the normalisation, from these control regions, bracketed the error in the absolute flux normalisation process. In addition, the 2.1% error in world average cross section was included into our error calculation.

5 Systematic Uncertainties

In what follows, we enumerate sources of systematic errors affecting the numerator. The muon identification-efficiency and energy-scale were the two most important measurables in the $\sigma^{CC}(\nu_\mu N)$ analysis. First, a precise understanding of the muon-chamber efficiency and stability was crucial. In a dedicated run in 1996 during the gap between the two neutrino spills from the SPS, we accumulated a large statistics of muons. This 'Flat-top μ' sample was identified by the veto-counter and the most upstream DCs. The energy spectrum of the Flat-top muon sample, spanning 4 to 50 GeV with a mean energy of 16 GeV, was similar to that induced by the ν_μ-CC events. The measured absolute efficiency of the μ-ID for this sample was 99.96%, in agreement with a detailed Monte Carlo simulation of the Flat-top muons. Next, we studied the stability of the μ-identification by using the fraction of events with an identified muon, $[\rho(\mu - ID)]$, as a function of time spanning 1995 through 1998, and as a function of 15 sections of the muon chambers. The $\rho(\mu - ID)$ was stable to better than 1% over this four-year period. The distribution of $\rho(\mu - ID)$, measured over 47 running periods, was consistent with a Gaussian distribution with an error in the mean of 0.15%. These consistency between data and MC simulation of μ-identification ensured the accuracy of the ν_μ-CC efficiency computed by the Monte Carlo.

In NOMAD, the E_μ-scale was determined by the accurately measured B-field and a precise DC-alignment accomplished by using several million beam muons traversing the detector throughout the neutrino runs. The momentum scale was checked by using the invariant mass (M_{K_S}) of over 30,000 reconstructed K_S^0 in the CC and NC data. For the K_S^0-momenta above 1 GeV (5 GeV), the data yielded 30,831 (13,765) K_S^0 with an average $M_{K_S} = 498.20 \pm 0.071$ MeV $(M_{K_S} = 498.80 \pm 0.100$ MeV); the corresponding MC, with a +0.25% shift in momentum, yielded 498.2 ± 0.059 MeV $(M_{K_S} = 498.80 \pm 0.090$ MeV). The error in the average was estimated by RMS $(=12$ MeV$)/\sqrt{N}$, where N was the number of K_S^0. In contrast, if the momentum were shifted by -0.5%, the MC would yield $M_{K_S} = 496.00 \pm 0.059$ MeV in disagreement with the data. The systematic error on the E_μ-scale was determined to be 0.2%.

Neutrino-induced hadron jets, including charged and neutral particle multiplicity and fragmentation, are poorly understood resulting in a discrepancy between the hadronic energy of data and MC. We reduced this discrepancy by correcting the simulated hadronic energy E_{HAD} by a constant factor κ_H, based on the distribution of $y_{Bj} = E_{HAD}/E_\nu = E_{HAD}/(E_{HAD} + E_\mu)$ in Monte Carlo and data. We relied on the precise measurement of E_μ. To determine the κ_H trials were made to minimize the χ^2 between data and MC y_{Bj}- and E_{HAD}-distributions, for events with $E_{HAD} \geq 2.5$ GeV, by varying κ_H from 0.9 to 1.1 in steps of 0.002 in the MC. The χ^2 was minimised at κ_H of 0.950, $i.e.$ the MC overestimated E_{HAD} by 5%. The comparison of the y_{Bj} distribution between data and the uncorrected-MC is shown in Figure 1(a), where $\frac{\chi^2}{DoF}$ is 795.1/49. The corresponding comparison after correcting the MC-E_{HAD} is shown in Figure 1(b), where $\frac{\chi^2}{DoF}$ is 89.6/49. To determine the error on κ_H we formed a 'scaled'-χ^2 which yielded the scaled-$\frac{\chi^2}{DoF}$ equal to unity at κ_H of 0.950. This was achieved by increasing the errors by 40%. Figure 1(c) shows the scaled-χ^2 as a function of κ_H. An increase of 1.0 from the minimum in the the scaled-χ^2 (see the inset) was used to set the uncertainty on the optimum κ_H value of 0.950. Additionally, the fiducial and kinematic cuts were varied and the range in κ_H was redetermined for unity variation in the scaled-χ^2. We concluded that an error of ± 0.006 bracketed the error on κ_H. Since κ_H was determined over the entire range of E_ν, to cover possible variations in κ_H as a function of E_ν, we increased the scale-error by 50%. Correcting E_{HAD} in the MC by κ_H also improved the agreement between the data and MC distributions of other kinematic variables: Q^2, W^2, and x_{Bj} where the improvement was comparable to that shown in Figure 1(b). The E_{HAD} correction factor determined in this analysis is closer to unity than the value of 0.93 used in our previous analyses [15] because of better tuning of the Monte Carlo and a reprocessing of the data that improved the reconstruction of high multiplicity events. The difference in the $\sigma^{CC}(\nu_\mu N)$ due to the ± 0.009 uncertainty on κ_H was computed and assigned as the systematic error. This systematic uncertainty would have to be a factor of 2.5 times larger to make it one of the dominant systematic errors in the analysis. Although the 0.9% error in the E_{HAD}-scale is adequate for the present inclusive $\sigma^{CC}(\nu_\mu N)$ measurement, efforts are underway to reduce this error to the 0.5% level using improved modeling [16] and analysis for the future ν_μ-CC differential cross-section as a function of E_ν, x_{Bj}, and y_{Bj}, and the weak mixing angle measurements. Table 2 lists the systematic errors on the $\sigma^{CC}(\nu_\mu N)/E_\nu$ as a function of visible energy.

Radiative corrections [17] that affected measurables, such as E_μ, θ_μ, and E_{HAD}, were folded into the $\sigma^{CC}(\nu_\mu N)$ measurement as a function of E_ν. The dominant radiative effect, typically less than 1% on σ/E_ν, occurred when a photon, radiated by the muon, was measured as part of the hadronic system. No other effort was made to correct the ν_μ-CC cross section to the Born-level.
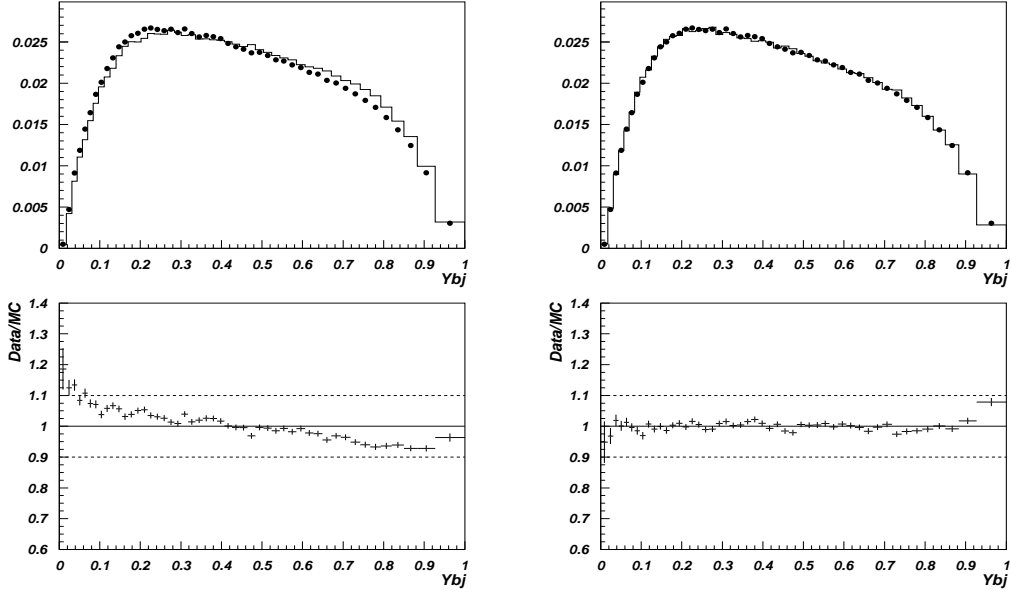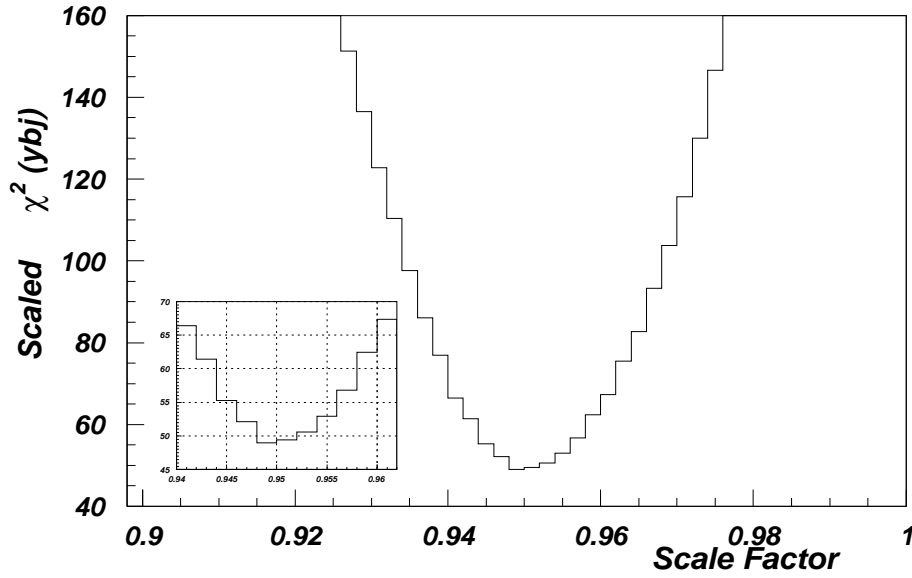
Fig. 1. The Data and MC y_{Bj}-Distributions: The y_{Bj} distributions for data(symbols) and MC(histogram) (a) before and (b) after rescaling E_{HAD} are shown in the top; the ratio of data to Monte Carlo for the two distributions are also shown. The lower plot (c) shows the scaled-χ^2 Distribution for y_{BJ} as a function of E_{HAD}-scale.

6 Result

After the E_{HAD}-scale correction, we present the E_{VIS} comparison between data and MC in Figure 2. Except for the lowest energy bin, the agreement

E_{vis} (GeV)	Relative Flux	Normalisation Region	μ-Acceptance	E_{HAD}-Scale	QE:RES:DIS
2.5–10	0.026	0.005	0.004	0.008	0.002
10–15	0.018	0.004	0.001	0.004	0.001
15–30	0.016	0.005	0.001	0.006	0.000
30–50	0.022	0.005	0.000	0.003	0.000
50–100	0.040	0.004	0.000	0.005	0.000
100–300	0.051	0.004	0.002	0.010	0.000

Table 2
Systematic Uncertainties on σ/E in E_ν-bins.

is better than 2% in the energy range shown. We point out that the ν_μ-CC cross-section was not modified in the Monte Carlo. The inclusive ν_μ-CC cross-sections were derived from this distribution. The final result of the measurement of the inclusive ν_μ charged current (CC) cross section is summarized in Table 3. The E_ν-bin, the average-E_ν, number of observed data and background (mainly from NC) events passing the selection criteria are listed respectively in the first four columns. The observed data are corrected by subtracting the background, and then dividing by the efficiency (5-column). The cross section, after correcting for non-isoscalarity, was calculated by dividing the corrected data (6-column) by the flux after absolute normalisation (7-column) and the average-E_ν. The $\sigma^{CC}(\nu_\mu N)/E_\nu$ with the statistical, systematic, and total errors are shown in the last four columns of Table 3.

The inclusive ν_μ CC cross section divided by E_ν is plotted as a function of E_ν in Figure 3 together with existing measurements. From this plot, agreement with the existing data above $E_\nu \geq 30$ GeV is seen: $\sigma^{CC}(\nu_\mu N)/E_\nu$ is flat above 30 GeV; it rises at lower energies due to the increasing presence of the non-scaling processes. In the sub 30 GeV region, the NOMAD measurements improve the precision. We note that in earlier publications on $\sigma^{CC}(\nu_\mu N)$, in the $2 \leq E_\nu \leq 30$ GeV region, such as by Baker et al. [18] and Anikeev et al. [20], the ν_μ-flux was constrained using QE events by selecting low-E_{HAD} events. The proponents then used the QE cross-section to deduce the flux, assuming that the QE cross-section was known to a $\pm 5\%$ precision. This, in our opinion, was an optimistic precision. A compilation of all the QE-measurements shows that the error on the QE cross-section, in the $2 \leq E_\nu \leq 30$ GeV range, is close to 15% as currently used by NOMAD in this paper and MINOS [21] collaborations.
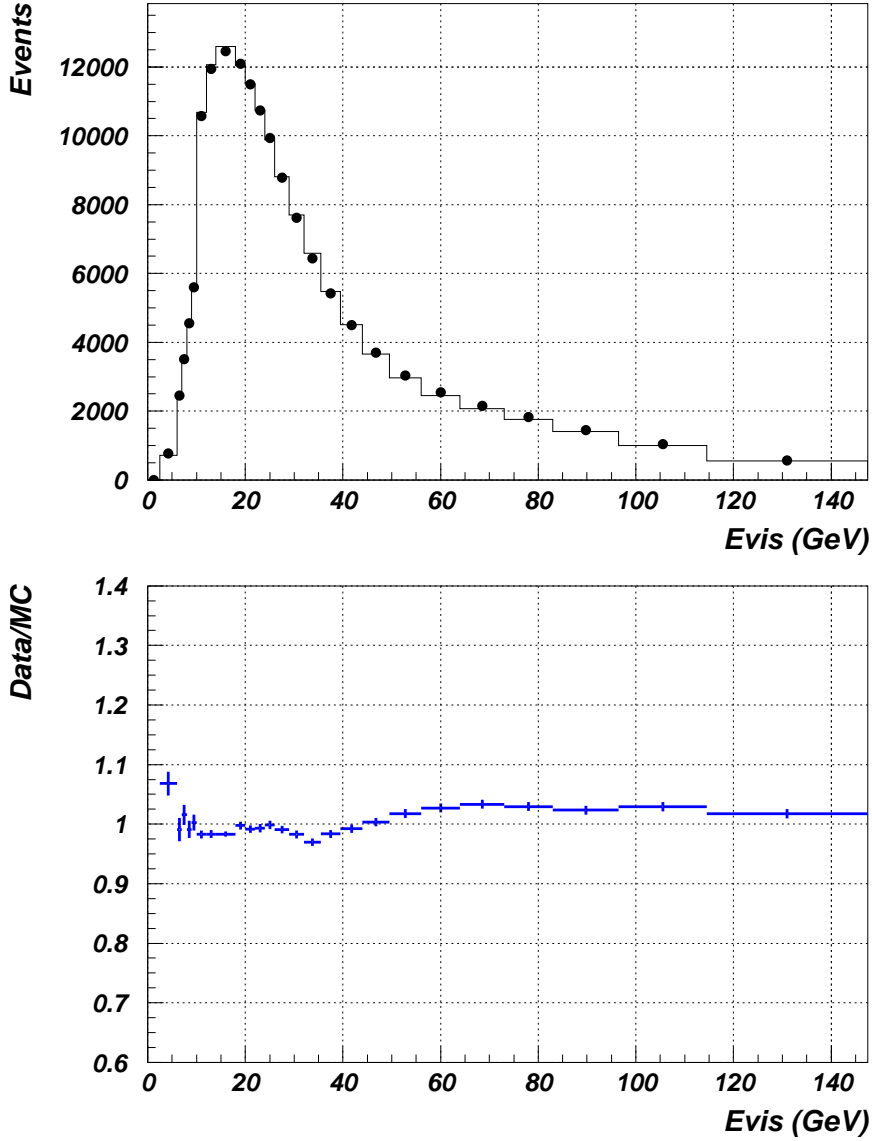
Fig. 2. Distributions of E_{VIS} for Data(symbols) and Monte Carlo (histogram): The E_{HAD} correction is applied to the MC. Only the statistical errors are shown. The ratio of data to Monte Carlo is also presented.
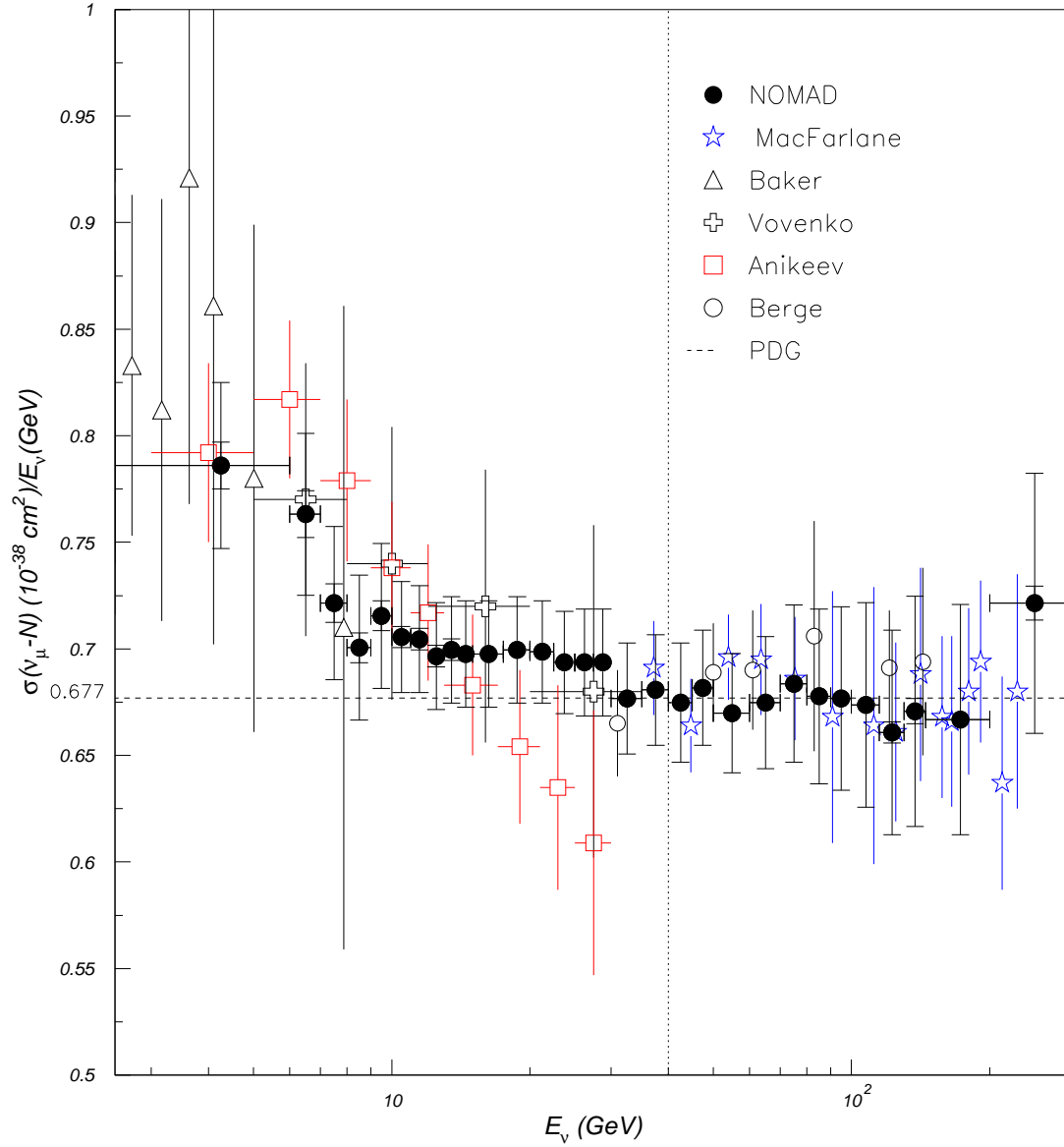
Acknowledgments

11

Fig. 3. Inclusive ν_μ-N Charge Current Cross Section -vs- E_ν: The $\sigma^{CC}(\nu_\mu N)/E_\nu$ is plotted as a function of E_ν, where N represents an iso-scalar nucleon within the the NOMAD target. The outer (inner) error bars show the total (statistical) error. Other measurements in this plot are by D.B.MacFarlane *et al.*[1], J.P. Berge *et al.*[2], N.J.Baker *et al.*[18], A.S. Vovenko *et al.*[19], and V.Anikeev *et al.*[20]. The region $E_\nu \geq 40$ GeV was used to normalize the $\sigma^{CC}(\nu_\mu N)/E_\nu$ to the asymptotic world average [3], shown as the dashed line, derived from high energy data.

12

$E_\nu - Bin$ (GeV)	$Avg.E_\nu$ (GeV)	Data	Bkgd	Eff.	Cor.Data	Flux (10^5)	σ/E_ν	Stat Err.	Syst Err.	Total Err.
2.5- 6.0	4.60	5429.0	51.2	0.409	13296.9	4.07	0.786	0.011	0.035	0.037
6.0- 7.0	6.50	4917.0	45.0	0.452	10778.5	2.40	0.763	0.011	0.036	0.038
7.0- 8.0	7.50	7011.0	53.2	0.445	15625.2	3.20	0.722	0.009	0.035	0.036
8.0- 9.0	8.50	9119.0	46.0	0.445	20369.0	3.79	0.701	0.007	0.033	0.034
9.0- 10.0	9.50	11192.0	50.5	0.443	25171.9	4.10	0.716	0.007	0.033	0.034
10.0- 11.0	10.50	20244.0	87.9	0.704	28629.3	4.29	0.706	0.005	0.026	0.026
11.0- 12.0	11.50	22051.0	91.2	0.698	31471.8	4.31	0.705	0.005	0.024	0.025
12.0- 13.0	12.50	23349.0	100.7	0.685	33936.8	4.33	0.697	0.005	0.024	0.025
13.0- 14.0	13.50	24433.0	94.3	0.686	35462.1	4.17	0.700	0.005	0.024	0.025
14.0- 15.0	14.50	24802.0	91.1	0.682	36249.3	3.98	0.698	0.004	0.025	0.025
15.0- 17.5	16.20	62447.0	249.7	0.678	91750.9	9.00	0.698	0.003	0.025	0.025
17.5- 20.0	18.70	60825.0	246.5	0.686	88315.5	7.48	0.700	0.003	0.025	0.025
20.0- 22.5	21.20	57249.0	240.2	0.690	82590.0	6.18	0.699	0.003	0.024	0.024
22.5- 25.0	23.70	51919.0	226.6	0.691	74772.6	5.04	0.694	0.003	0.024	0.024
25.0- 27.5	26.20	46696.0	233.4	0.693	67054.3	4.09	0.694	0.003	0.025	0.025
27.5- 30.0	28.70	41462.0	239.3	0.696	59235.3	3.30	0.694	0.003	0.025	0.025
30.0- 35.0	32.30	68858.0	431.4	0.708	94730.8	4.91	0.677	0.003	0.026	0.026
35.0- 40.0	37.30	54059.0	420.5	0.704	75291.1	3.33	0.681	0.003	0.026	0.026
40.0- 45.0	42.40	43650.0	379.9	0.715	61212.5	2.35	0.675	0.003	0.028	0.028
45.0- 50.0	47.40	36135.0	326.3	0.718	49084.9	1.71	0.682	0.004	0.027	0.027
50.0- 60.0	54.60	57357.0	618.2	0.733	77653.8	2.35	0.670	0.003	0.028	0.028
60.0- 70.0	64.70	45880.0	509.8	0.733	61753.1	1.57	0.675	0.003	0.031	0.031
70.0- 80.0	74.80	38523.0	409.6	0.700	54226.5	1.18	0.684	0.003	0.037	0.037
80.0- 90.0	84.80	32054.0	309.1	0.666	47043.6	0.92	0.678	0.004	0.041	0.041
90.0-100.0	94.80	25884.0	231.8	0.636	39517.5	0.70	0.677	0.004	0.043	0.043
100.0-115.0	107.00	29673.0	258.4	0.628	46821.5	0.72	0.674	0.004	0.048	0.048
115.0-130.0	122.00	20327.0	176.7	0.608	32923.4	0.46	0.661	0.005	0.048	0.048
130.0-145.0	136.90	14204.0	117.7	0.583	24337.2	0.29	0.671	0.006	0.054	0.054
145.0-200.0	165.90	24007.0	170.9	0.545	43805.8	0.44	0.667	0.004	0.054	0.054
200.0-300.0	228.30	8589.0	56.0	0.496	17183.5	0.12	0.721	0.008	0.060	0.061

Table 3
Summary of the ν_μ-CC Cross Section, $\sigma(10^{-38}cm^2)/E(GeV)$, Analysis: The fifth-column represents the efficiency folded with the acceptance, see Section 3. The σ/E_ν is presented for an iso-scalar nucleon within the NOMAD target.

References

[1] R. Blair *et al.*, Phys. Rev. Lett 51, 343 (1983), D.B. MacFarlane *et al.*, Z. Phys. C26, 1 (1984)

[2] J.P. Berge *et al.*, Z.Phys.C35:443,1987.

[3] Journal of Physics G33, 336 (2006)

[4] G. Acquistapace *et al.*, CERN-ECP/95-14

[5] P. Astier *et al*., NIM A515, 800-828 (2003)

[6] P. Astier *et al*., Nucl. Phys. B611, 3-39 (2001)

[7] J. Altegoer *et al*., NIM A404, 96-128 (1998)

[8] M. Anfreville *et al.*, Nucl. Instrum. Meth. A **481** (2002) 339

[9] G.Ingelman *et al*., Comput. Phys.Comm, 101, 108-134(1997)

[10] T.Sjöstrand, Comput. Phys.Comm, 82, 74-90(1994)

[11] R.Brun *et al*., CERN Program Library, W5013, 1993.

[12] M. Glück, E. Reya, A. Vogt, Z. Phys. C 53 127 (1992)

[13] G. Ambrosini *et al*., Eur. Phys. J., C 10 (1999) 605-627

[14] H.W. Atherton *et al*., CERN Yellow Report 80-07, 1980.

[15] P. Astier *et al*., Phys. Lett. B **570**, 19 (2003)

[16] S. Kulagin and R.Petti, Nucl. Phys. A 765 (2006) 126-187; S. Alekhin, S. Kulagin and R. Petti, NuInt07, arXiv:hep-ph/0710.0124; S. Kulagin and R. Petti arXiv: hep-ph/0703033

[17] A.B. Arbuzov, D.Y. Bardin and L.V. Kalinovskaya, JHEP 0506, 078 (2005)

[18] N.J. Baker *et al*., Phys. Rev. D25, 617 (1982)

[19] A.S. Vovenko *et al*., Sov. J. Nucl. Phys. 30, 527 (1979)

[20] V.B. Anikeev *et al*., Z. Phys. C70, 39 (1996)

[21] D.G. Michael *et al*., Phys.Rev.Lett.97 (2006) 191801; a detailed version of the result is submitted to Phys.Rev.D.